International Journal of
INTELLIGENT SYSTEMS AND APPLICATIONS IN ENGINEERING
ISSN:2147-6799 www.ijisae.org Original Research Paper

Energies of Cuprous Oxide Nanofilms and Annealing Temperature Effect on Structural and Dispersion Properties using Fuzzy Logic

Inass Abdulah Zgair [1], Abdulazeez O. Mousa Al-Ogaili[1], Khalid Haneen Abass[2]

Submitted: 22/08/2023 **Revised**: 09/10/2023 **Accepted**: 20/10/2023

Abstract: Solar cell fabrications need films with nanostructure without defects, which can achieve at a quantum dot or fine grain size. The structural, optical characteristics, and energies of the films of as-grown and annealed Cuprous Oxide (Cu_2O) were deposited onto glass substrates via the thermal evaporation technique were studied. The average crystal size of the nanofilms was increased from 12 nm to 16 nm after annealing at 200 ºC, while the dislocation density was decreased. The consequence displays that the fabricated films had transmittance at UV- region of more than 98% and the shift of absorption edge was towards a longer wavelength after the annealing process. The value of the direct band gap of as-deposited Cu_2O thin film was 2.57 eV and it decreased to be 2.15 eV for annealed films. Volume Loss Energy Function and Surface Loss Energy Function and dispersion parameters such as single oscillator energy (E_o), Dispersion energy (E_d), static refractive index (n (0)), and Moments (M_{-1} and M_{-3}) were studied to determine the suitable applications such as solar cell, optoelectronic and optical devices, or in communications using Fuzzy Logic.

Keywords: *Nanofilm, Thermal Evaporation, Cuprous Oxide, Fuzzy Logic.*

1. Introduction

Cuprous Oxide (Cu_2O) has acquired renewed attention for numerous technological applications as a result of its optoelectronic characteristics [1,2]. The space group that Cu_2O belongs to is Pn3m were the unit cell has four oxygen in addition to two copper ions. These are organized with oxygen atoms in a lattice of a body center cubic enclosed tetrahedrally by ions of copper [3]. Cu_2O is a good photovoltaic material due to, its availability of Cu material on earth, theoretical energy conversion efficiency, which is nearly 20% in addition to nontoxicity, inexpensive to produce, and in the visible regions it is have high absorption coefficient with a direct band gap of approximately 2.1 eV [4,5], while with very fine particles of nanofilms, the energy gap will increase widely to reach more than 3.5 eV (in the case of a quantum dot) [6]. The large-scale band gap of some metal oxides restricts the absorption of light in the ultraviolet range, lead to decrease in utilizing sunlight, which make it an important photocatalyst material for many applications especialy solar energy conversion [7].

Cu_2O had a considerable interest for decades, owing mostly to its possible uses in Lithium-ion batteries [8], nano-magnetic devices [9], photocatalysis [10], transistors [11], gas sensors [12], photodetector [13], and in the solar cell [14,15]. In this work, the Cu_2O nanostructure films were fabricated via thermal evaporation technique and annealed at 200 ºC to prepare films with fine surfaces and small particle sizes to candidate them for solar cell, optoelectronic, and optical application.

2. Experimental

The deposition of Cuprous oxide (Cu_2O) films was carried out by thermal evaporation method with a pressure of around 1×10^{-7} mbar and coated onto a pre-cleaned glass substrate. Before the evaporation process, ultrasonically the glass substrates have been cleaned by utilizing, acetone, ethanol, and distilled water. An Edwards (Edwards Auto 306) coating plant has been used. In the vacuum chamber, the distance that separate the substrate and source which is the Cu_2O powder was kept at 15 cm and the rate of deposition is approximately 0.3 nm/s after that the Cu_2O samples were annealed at 200 °C for 2h. An X-ray diffractometer utilized to studied the crystalline structure is (XRD, (Shimadzu-6000)) via Cu Kα with (λ= 1.5406 Å). UV–Vis spectrophotometer (Model, MEGA-2100- SCINCO) has been used to examine the optical characteristics in the range of (300–1200) nm of wavelength.

3. Results and Methods using Fuzzy logic

Patterns of X-ray diffraction (XRD) of Cu_2O nanofilms are presented in Fig. 1 (part (a) for as-deposited and (b) for annealed film at 200 ºC). The average size of crystals could be calculated using Scherer's formula [16,17]:

[1]*Department of Physics, College of Science, University of Babylon, Babel, Iraq*
[2]*Department of Physics, College of Education for Pure Sciences, University of Babylon, Babel, Iraq*
E-mail: inass.taha.scihigh65@student.uobabylon.edu.iq
E-mail: sci.abdul.azeez@uobabylon.edu.iq
E-mail: pure.khalid.haneen@uobabylon.edu.iq

$$D = \frac{0.9\,\lambda}{\beta\ COS\theta} \qquad (1)$$

where λ denoted to X-ray's wavelength used, β signified to (FWHM) which is abbreviation to (full-width at half-maximum) of the peak of diffraction and θ° denoted to Bragg's angle.

The dislocation density (δ), has been evaluated using the formula of Williamson and Smallman's and is represented as the number of lines of dislocation per unit volume [18].

$$\delta = \frac{1}{D^2} \qquad (2)$$

The micro-strain (Ɛ) of Cu_2O NPs films has been determined by the following formula [19]:

$$\varepsilon = \frac{\beta\cos\theta}{4} \qquad (3)$$

The XRD patterns for as prepared and annealed (T= 200◦C) Cu2O/glass nano films are displayed in Fig.(1a and b). A poly-crystalline structure with an orthorombic phase was discernible in the produced films, All Cu_2O thin films have characteristic peaks that correspond well with standard crystallographic data (01-075-1531). The preferred peaks of diffraction are (110), (220) and (310) plane for deposited samples as shown in Fig.(1b), the annealing operation increased the crystallinity of the film, and the peak intensity enhanced dramatically and become a sharper and so more intense. As the average crystal size increased, the dislocation density and the micro-strain have been reduced when annealed at 200 °C as listed in Table (1). This might be owing to the enhancement of the crystallinity of Cu_2O NPs films by the annealing process and the decrease in its crystal imperfections by offering the atoms enough energy to rearrange themselves in the lattice, thereby minimizing the random distribution of atoms inside the substance of the thin film using fuzzy logic also [20].

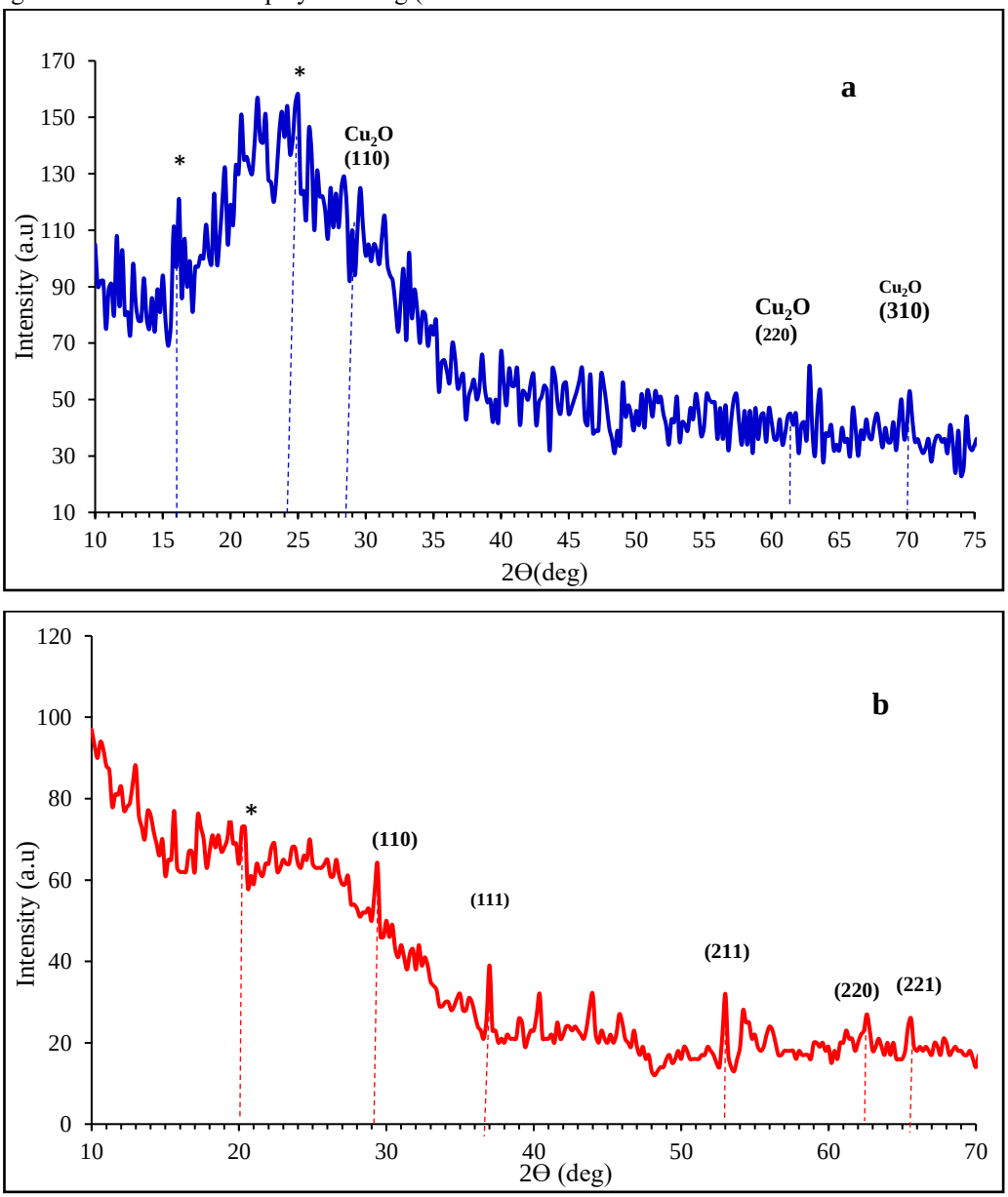

Fig.1: XRD pattern of Cu_2O nanofilms a) as-deposited and b) annealed at 200 ºC.

Samples	2Θ(deg)	FWHM	(hkl)	Average Crystal Size (nm)	$\delta=1/D^2$	Average micro-strain
Cu_2O nanofilm as deposited	16.17	0.611	-----	12	0.006944	0.139242
	29.634	0.585	-110			
	62.738	0.516	-220			
	70.214	0.754	-310			
Cu_2O nanofilm as annealed at 200°C	20.158	0.55	-----	16	0.003906	0.126596
	29.238	0.383	-110			
	36.974	0.397	-111			
	52.871	0.559	-211			
	62.648	0.652	-220			
	65.559	0.641	-221			

Table (1): The XRD data of Cu_2O nanofilms.

Fig.2 demonstrated the transmittance spectra of Cu_2O samples as a function of photon wavelength. The value of transmittance of Cu_2O nanofilms is relatively high up to 98% and around 96% for fabricated and annealed samples respectively, whereas noticeable the value of transmittance of Cu_2O thin films is slightly reduced after the annealing process.

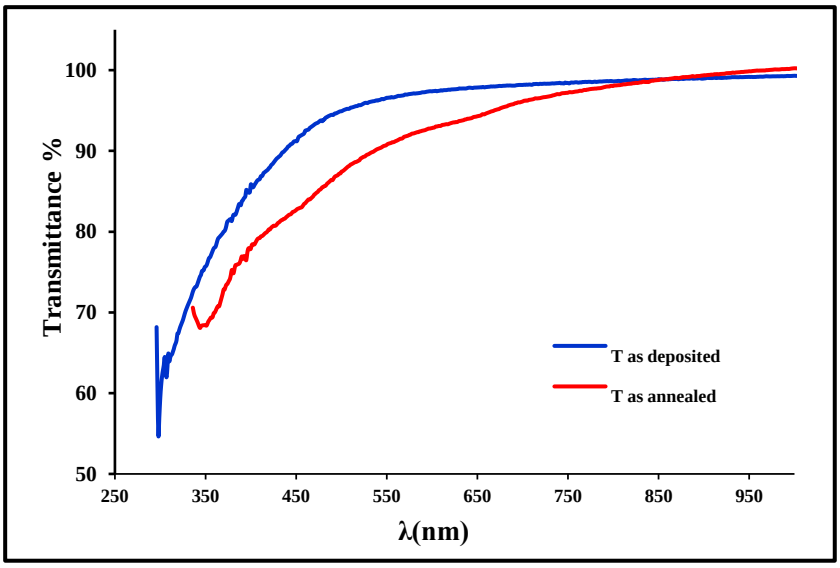

Fig. 2. Transmittance spectra of Cu_2O nanofilms as deposited and annealed at 200 °C.

In the UV–Vis absorbance spectra, the absorption edge exhibit (red shifts) towards the higher wavelengths after the annealing process as shown in Fig. 3.

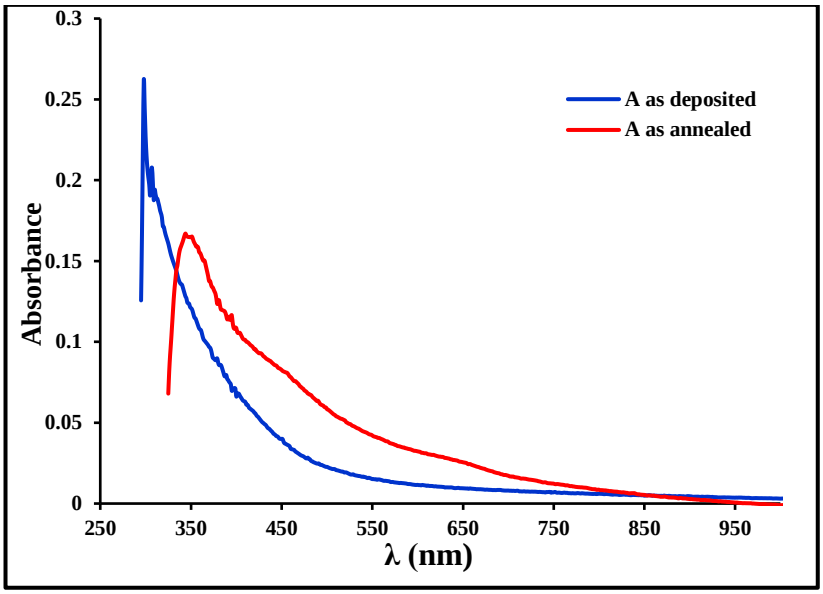

Fig. 3. Absorbance spectra of Cu_2O nanofilms as deposed and annealed at 200 °C.

Optical properties of Cu_2O NPs films grown on glass substrate by thermal evaporation and annealed at 200 °C. The linear relationship of the plot (hυ) versus $(\alpha h\upsilon)^2$ can be employed to evaluate the optical band gap based on the Tauce formula [21] and as displayed in Fig. 4 [32][33].

$$\alpha h\upsilon = B(h\upsilon - E_g)^n \quad (4)$$

where α denoted to the coefficient of absorption, B is a constant and E_g is denoted by the optical band gap. From the consequences, the value of Eg as-deposited films was 2.57 eV then decrease to be 2.15 eV for annealed samples. This result is approximately close to that evaluated by Wisz *et al.*,[22] and Oudah *et al.*, [23]. Whereas the standard energy gap of CdTe was 1.5 eV, the high variation in the values refers to the quantum confinement effect of the material. The confinement effect indicates of wide energy gap as a result of a semi-continuous recognized electronic state.

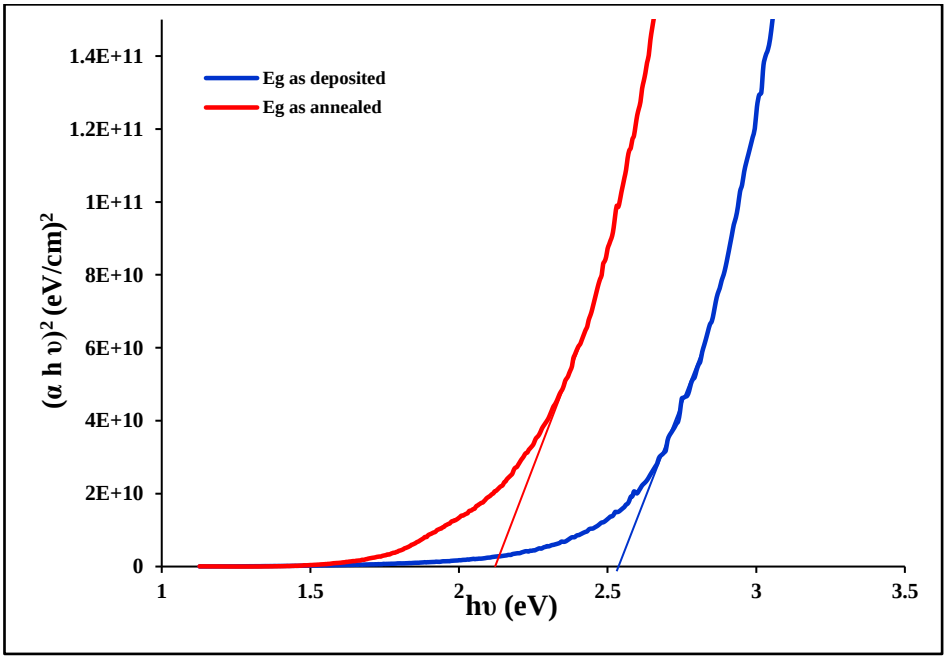

Fig. 4. Direct energy band gap of Cu_2O nanofilms as- deposited and after annealed at 200 °C.

(α) is the absorption coefficient which could be computed from the spectrum of absorbance utilizing the equation [24]:

$$\alpha = {}^{2.303\,A}/_{t} \quad (5)$$

where A denoted the absorbance and t represent the thickness.

The index of refraction (n) of Cu_2O NPs/glass thin film can be evaluated using the equation [25,26]:

$$n = \frac{1+\sqrt{R}}{1-\sqrt{R}} \quad (6)$$

where R denoted to the reflectance

From Fig.(5 and 6) can be seen that the absorption coefficient and refractive index decreased gradually and shifted toward lower energy after annealing the samples.

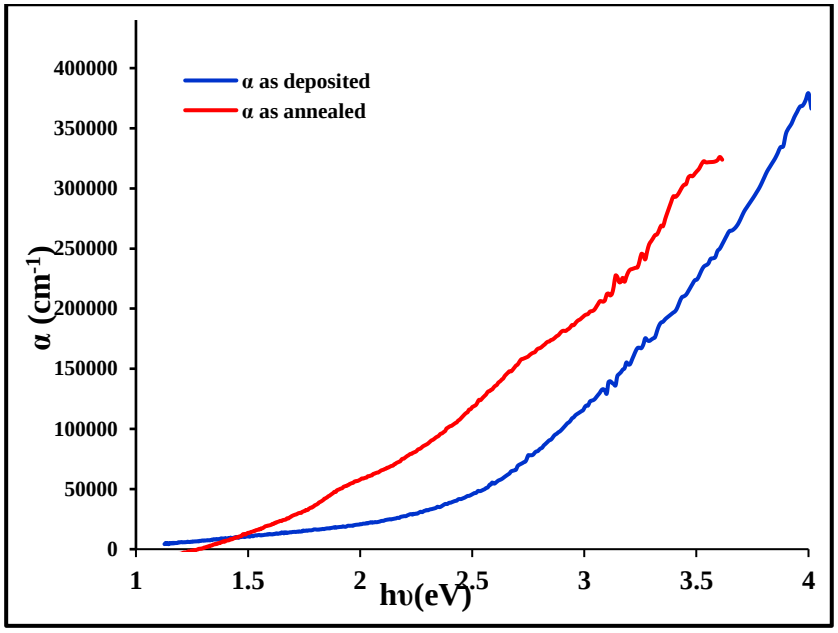

Fig. 5. Absorption coefficient of Cu_2O nanofilms as deposited and annealed at 200 ºC.

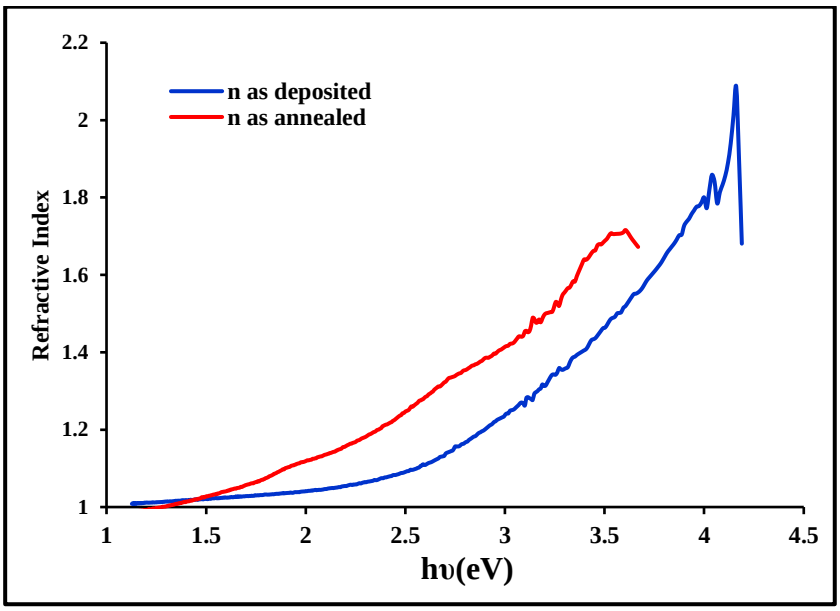

Fig. 6. Refractive index of Cu_2O nanofilms as deposited and annealed at 200 ºC.

The energy loss by electrons when traveling through the bulk and material's surface represented by the Volume Loss Energy Function (VLEF) and Surface Loss Energy Function (SELF) can be investigated from the following formulas [27]:

$$VELF = \frac{\varepsilon_i}{(\varepsilon_r + 1)^2 + \varepsilon_i^2} \quad (7)$$

$$SELF = \frac{\varepsilon_i}{\varepsilon_r^2 + \varepsilon_i^2} \quad (8)$$

where ε_r and ε_i are represent the real and imaginary part of dielectric constant respectively.

Figures (7) and (8) show Volume Loss Energy Function (VLEF) and Surface Loss Energy of deposited and annealed samples [34][35].

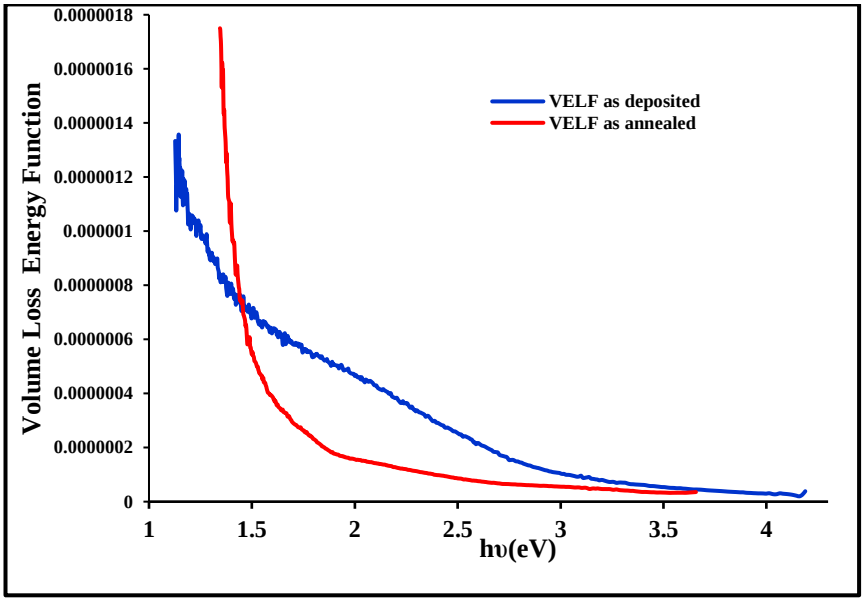

Fig. 7. Volume Loss Energy Function of Cu_2O nanofilms as deposited and annealed at 200 ºC.

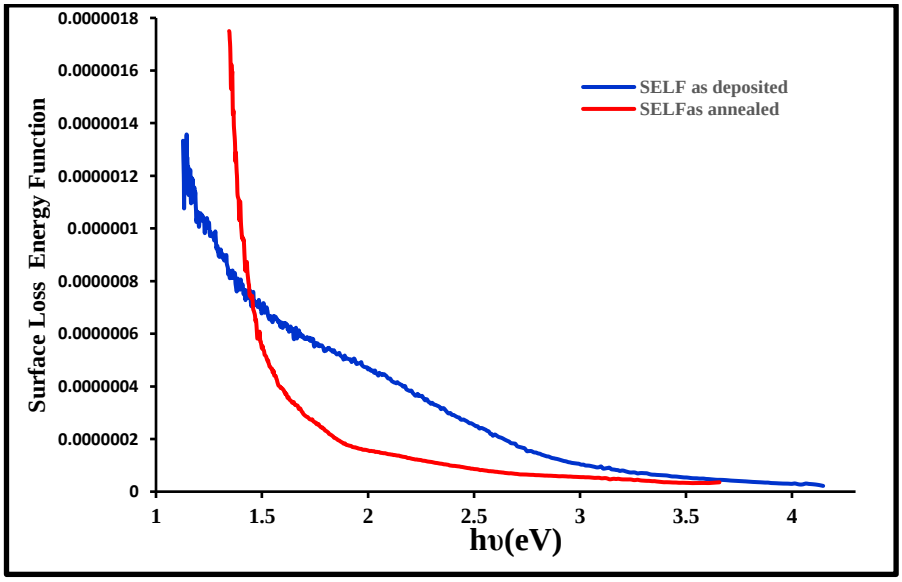

Fig. 8. Surface Loss Energy Function of Cu_2O nanofilms as deposited and annealed at 200 ºC.

The Wemple-DiDomenico model was used to present the parameters of dispersion for Cu_2O nanofilms using the relation [27,28].

$$(n-1)^{-1} = \frac{E_\circ^2 - (h\nu)^2}{E_d E_\circ} \qquad (9)$$

Where where n, E_o,E_d are refractive index, oscillator energy, and dispersion energy respectively [38][39].

This formula can be expressed graphically by drawing the refractive index factor $(1/(n^2 1))$ versus squared of photon energy $(hv)^{\wedge 2}$ as illsetratedi n Fig. (11) and Fig. (12). The straight line represents a slope that equal to $(1/ E_oEd)$, while the value of (E_o/E_d) can be obtained from intercepts the y-axis and the values of E_o and E_d reduce after annealing at 200°C. The value of optical band gap could be gotten from the formula Eo ≈2 Eg [29], which is reduced after annealing process, and this consequence can comparable with that obtained from Tauc model . The calculated E_o, E_d and E_g values were tabulated in Table 3. Another parameter of the Cu_2O NPs/glass films which are moments (M_{-1} and M_{-3}) of the optical spectra could be calculated via the equations [30,31]:

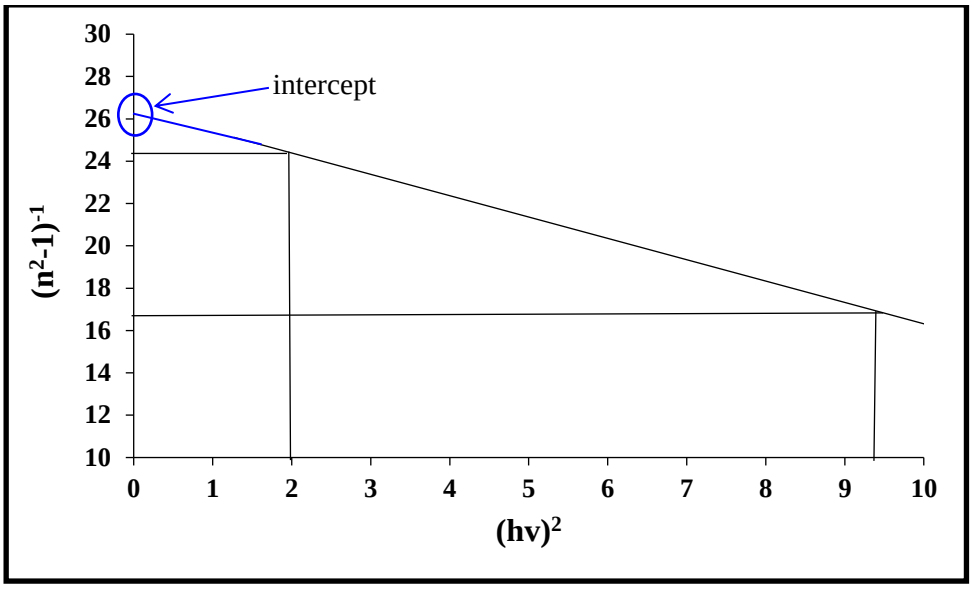

Fig.9. The 1/(n^2 -1) versus (hυ)^2 of Cu_2O nanofilm as deposited.

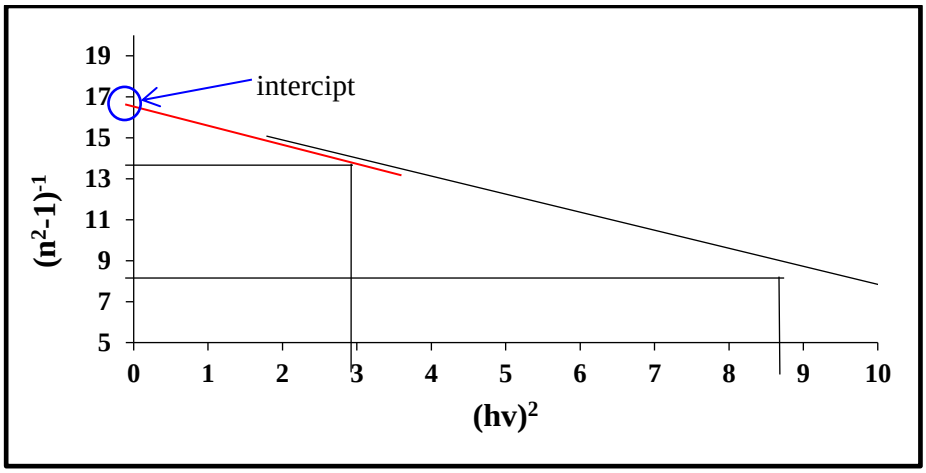

Fig.10. The 1/(n^2 -1) versus (hυ)^2 of Cu_2O nanofilm annealed at 200 ºC.

$$E_o^2 = \frac{M_{-1}}{M_{-3}} \quad (10)$$

$$E_d^2 = \frac{M_{-1}^3}{M_{-3}} \quad (11)$$

Table (2) show the increase of moments value (M_{-1} and M_{-3}) of optical spectra as well as $n_o(0)$ value after annealing process [36][37].

Table 2**:** The dispersion parameter of Cu_2O NPs/glass thin films.

Parameters	Cu_2O NPs as deposited	Cu_2O NPs annealed at 200 °C
E_o	5.177317393	4.38675693
E_g	2.588658696	2.193378465
E_d	0.197607534	0.261116484
$n^2(0)$	1.038167939	1.05952381
$n_o(0)$	1.018905265	1.02933173
ε	1.038167939	1.05952381
M_{-1}	0.038167939	0.05952381
M_{-3}	0.001423932	0.003093168

4. Conclusions

In this study, Cu_2O NPs thin films were successfully fabricated by way of the thermal evaporation technique. From XRD can be notice there is an increase in average crystal and the nanofilm have polycrystalline in nature. The direct energy gap of deposited Cu_2O NPs films were found to be 2.57 eV and around 2.15 eV when annealed at 200 °C. Parameters of Dispersion like E_o, E_d, n(0), M_{-1}, and M_{-3} are evaluated by utilizing the Wemple-DiDomenico model and the values of these parameters increase after annealing process.

References

[1] S. S. Sawant, A. D. Bhagwat and C. M. Mahajan , Synthesis of Cuprous Oxide (Cu_2O) Nanoparticles–a Review, Journal of Nano- and Electronic Physics , Vol. 8 No 1, pp.01035 (1-5), 2016

[2] C. Jayathilaka, L. S. R.Kumara , K. Ohara, C. Song, S. Kohara , O. Sakata, W. Siripala and S. Jayanetti, Enhancement of Solar Cell Performance of Electrodeposited Ti/n-Cu_2O/p-Cu_2O/Au Homojunction Solar Cells by Interface and Surface Modification, Crystals, Vol.10, No.609,pp.1-14,2020

[3] K.U. Isah, M.Bakeko, U. Ahmadu, U. E.Uno, M. I. Kimpa and J. A. Yabagi, Effect Of Oxidation Temperature on the Properties of Copper Oxide Thin Films Prepared from Thermally Oxidised Evaporated Copper Thin Films, IOSR Journal of Applied Physics, Vol. 3, Issue 2 ,pp. 61-66, 2013.

[4] V.A. Gevorkyan, A. E. Reymers, M N Nersesyan and M A Arzakantsyan, Characterization of Cu_2O Thin Films Prepared by Evaporation of CuO Powder, International Symposium on Optics and its Applications (OPTICS2011), Vol.350,pp.012027 (1-6), 2012.

[5] M. Umar, M. Y. Swinkels, M. De Luca, C. Fasolato, L. Moser, G.Gadea, L.Marot, T. Glatzel and I. Zardo, Morphological and Stoichiometric Optimization of Cu_2O Thin Films by Deposition Conditions and Post-Growth Annealing, Thin Solid Films, Vol. 732, p. 138763 (1-11), 2021.

[6] Abbas and K. H. Abass, Nano-Layers of Cu_2O Prepared by Thermal Evaporation Technique: Morphology and Optical Properties , Materials Today: Proceedings, Vol.60 .pp. 1402–1408, 2022.

[7] A.N. Tuama, K.H.Abbas, , M.Q., Hamzah, S.O.Mezan, , A.H.Jabbar and M.A. Agam, An Overview on Characterization of Silver/Cuprous Oxide Nanometallic (Ag/Cu_2O) as Visible Light Photocatalytic, International Journal of Advanced Science and Technology, Vol. 29,No.3, pp. 5008-5018, 2020.

[8] H.M. Wei, H.B. Gong, L. Chen, M. Zi and B.Q. Cao, Photovoltaic Efficiency Enhancement of Cu_2O Solar Cells Achieved by Controlling Homojunction Orientation and Surface Microstructure, J. Phys. Chem. C,Vol. 116,No.19,pp. 10510–10515,2012.

[9] Y. Bai, T. Yang, Q.Gu, G. Cheng and R. Zheng , Shape Control Mechanism of Cuprous Oxide Nanoparticles in Aqueous Colloidal Solutions,Powder Technology ,Vol.227 ,pp. 35–42, 2012.

[10] A. hssi, L. Atourki, K. Abouabassi, A. Elfanaoui, K. Bouabid1, A. Ihlal,S. Benmokhtar and M. Ouafi , Growth and Characterization of Cu_2O for Solar Cells Applications, AIP Conference Proceedings,Vol. 2056,pp. 020006 (1-6), 2018.

[11] G. Salek, C. Tenailleau, P. Dufour and S. Guillemet-Fritsch, Room Temperature Inorganic Polycondensation of Oxide (Cu_2O and ZnO) Nanoparticles and Thin Films Preparation by the Dip-Coating Technique, Thin Solid Films, Vol. 589. pp. 872-876,2015

[12] O. Lupan, V. Cretu, V. Postica, N. Ababii, O. Polonskyi, V. Kaidas, F. Schütt, Y. K. Mishra, E. Monaico, I. Tiginyanu, V. Sontea, T. Strunskus, F. Faupe and R. Adelung, Enhanced Ethanol Vapour Sensing Performances of Copper Oxide Nanocrystals with Mixed Phases, Sensors and Actuators B: Chemical,Vol. 224,pp. 434–448, 2016.

[13] W-J. Lee and X-J. Wang , Structural, Optical, and Electrical Properties of Copper Oxide Films Grown by the SILAR Method with Post-Annealing, Coatings,Vol. 11,No. 864,pp.1-13,2021.

[14] S. Siol, C.J. Hellmann, S.D. Tilley, M. Gr¨atzel, J. Morasch, J. Deuermeier, W. Jagermann and A. Klein, Band Alignment Engineering at Cu_2O/ZnO Heterointerfaces, ACS Appl. Mater. Interfaces, Vol. 8, No.33, pp.21824–21831, 2016.

[15] N. Tuama, K. H. Abass and M. A. Agam, Fabrication and Characterization of Cu_2O:Ag/Si Solar Cell Via Thermal Evaporation Technique, International Journal of Nanoelectronics and Materials Vol. 13, No. 3, p.p 601-614, 2020.

[16] M. Birkholz ,P. F. Fewster and C. Genzel, Thin Film Analysis by X-Ray Scattering, Wiley-Vch Verlag Gmb H and Co. KGaA,Weinheim, 2006

[17] S.R. Elliott, Physics of Amorphous Materials, Long Man Group Limited, UK, 1983.

[18] K. Dhanabalan, A.T. Ravichandran, A.Vasuhi, R. Chandramohan, P. Karthick, and S.Mantha, Effect of Annealing based on the Structural, Optical, Morphological and Antibacterial Activities of Copper Oxide Thin Films by SILAR Technique, Int. J. Thin Film. Sci. Tec.,Vol. 11, No. 1, pp. 65-72, 2022.

[19] M. R. Johan , M.S. M. Suan, N. L. Hawari and H. A. Ching, Annealing Effects on the Properties of Copper Oxide Thin Films Prepared by Chemical Deposition, Int. J.Electrochem. Sci.,Vol. 6 ,pp.6094 – 6104,2011.

[20] Akgul , G. Akgul , N. Yildirim, H. E. Unalan ,R.Turan, Influence of thermal annealing on microstructural, morphological, optical properties and surface electronic structure of copper oxide thin films, Materials Chemistry and Physics,Vol. 147 ,p987e995, 2014.

[21] J. I. Pankove, Optical Process in Semiconductors, Dover Publishing, Inc., New York,1971.

[22] G. Wisz, P. Sawicka-Chudy, P. Potera, M. Sibiński, R. Yavorskyi, Ł. Głowa, B.Cieniek and M. Cholewa, Morphology, Composition, Structure and Optical Properties of Thermally Annealed Cu_2O Thin Films Prepared by Reactive DC Sputtering Method, Molecular Crystals and Liquid Crystals, Vol. 672, No. 1,pp. 81–91, 2018

[23] M. H. Oudah, M. H. Hasan, A. N. Abd, Some Physical Properties of Copper Oxide Thin Films Prepared by Electrolysis Method, World Scientific News ,Vol.135,pp.59-70, 2019.

[24] S. M. Sze and K. K. Ng, Physics of Semiconductor Devices, Second Edition, John Wiley and Sons, Inc. , 2002.

[25] S. Mahmoud, Optical Properties of Tin in the 2.5 to 40 μm region, J. Mater. Sci, Vol.22, pp.251-256,1987.

[26] A. K. Zbala, A. O. Mousa Al-Ogaili and K. H. Abass, Optical Properties and Dispersion Parameters of PAAm-PEG Polymer Blend Doped with Antimony (III) Oxide Nanoparticles, NeuroQuantology, Vol. 20,No.2, pp. 62–68, 2022.

[27] H. R. A. Mohammed, A. O. Mousa Al-Ogaili and K. H. Abass, Synthesis and Structural Characterization of Nano-Layers Prepared from Al-Ni-Cr Alloy for Reflectance Coatings, AIP Conference Proceedings, 2398,p. 020039, 2022

[28] K.H. Abass, A. Adil and M.K. Mohammed, Fabrication and enhancement of SnS:Ag/Si solar cell via Thermal Evaporation Technique, Journal of Engineering and Applied Sciences, Vol.13,No.4, pp. 919-925, 2018.

[29] S.H. Wemple, DiDomenico; Oxygen Octahedr Ferroelectrics. Theory of Electro-Optical and Non Linear Optical Effects, J. Appl. Phys., 40, 720, 1969.

[30] K. H. Abass, M. H. Shinen and A.F.Alkaim, Preparation of TiO_2 nanolayers via. Sol-Gel Method and Study the Optoelectronic Properties as Solar Cell Applications, Journal of Engineering and Applied Sciences,Vol. 13,No.22, pp. 9631-9637, 2018.

[31] A. Ahmed , M. H. Eisaa, and M. D. Abdulla, Study the Optical Parameters of Aluminum Doped ZnS Films Deposited on Soda-Lime Glass Substrate, Chalcogenide Letters, Vol. 19, No. 9, pp. 591 - 598, 2022

[32] S. Hassanien and I. Sharma, Optical Properties of Quaternary a-Ge15-x Sbx Se50 Te35 Thermally Evaporated Thin-Films: Refractive Index Dispersion and Single Oscillator Parameters, Optik - International Journal for Light and Electron Optics ,Vol.200 ,p. 163415, 2020.

[33] Z.M. Jawad and K. H. Abass, Fabrication and Study the Optical Properties and Dispersion Parameters of PVA/PAAm with CuNW Additive, NeuroQuantology, Vol. 20, No.2, p.p 87-95, 2022.

[34] Mall, Pawan Kumar, et al. "Rank Based Two Stage Semi-Supervised Deep Learning Model for X-Ray Images Classification: AN APPROACH TOWARD TAGGING UNLABELED MEDICAL DATASET." Journal of Scientific & Industrial Research (JSIR) 82.08 (2023): 818-830.

[35] Narayan, Vipul, et al. "A Comprehensive Review of Various Approach for Medical Image Segmentation and Disease Prediction." Wireless Personal Communications (2023): 1-30.

[36] Mall, Pawan Kumar, et al. "A comprehensive review of deep neural networks for medical image processing: Recent developments and future opportunities." Healthcare Analytics (2023): 100216.

[37] Narayan, Vipul, et al. "Severity of Lumpy Disease detection based on Deep Learning Technique." 2023 International Conference on Disruptive Technologies (ICDT). IEEE, 2023.

[38] Awasthi, Shashank, et al., eds. AI and IoT-based Intelligent Health Care & Sanitation. Bentham Science Publishers, 2023.

[39] Sanyal, Goutam, et al., eds. International Conference on Artificial Intelligence and Sustainable Engineering: Select Proceedings of AISE 2020, Volume 1. Vol. 836. Springer Nature, 2022.

[40] Ranjan, Roop, et al. "A Manifold-Level Hybrid Deep Learning Approach for Sentiment Classification Using an Autoregressive Model." Applied Sciences 13.5 (2023): 3091.

[41] Rai, Ashok Kumar, and A. K. Daniel. "FEEC: fuzzy based energy efficient clustering protocol for WSN." International Journal of System Assurance Engineering and Management 14.1 (2023): 297-307.

[42] Botha, D., Dimitrov, D., Popović, N., Pereira, P., & López, M. Deep Reinforcement Learning for Autonomous Robot Navigation. Kuwait Journal of Machine Learning, 1(3). Retrieved from

http://kuwaitjournals.com/index.php/kjml/article/view/140

[43] Dasari, S. ., Reddy, A. R. M. ., & Reddy , B. E. . (2023). KC Two-Way Clustering Algorithms For Multi-Child Semantic Maps In Image Mining. International Journal on Recent and Innovation Trends in Computing and Communication, 11(2s), 01–11. https://doi.org/10.17762/ijritcc.v11i2s.6023